Metallurgical and Materials Engineering *Research paper*
Association of Metallurgical Engineers of Serbia AMES *https://doi.org/10.30544/722*

NUMERICAL INVESTIGATION OF RESIDUAL STRESSES IN WELDED JOINTS OF CYLINDRICAL SHELL

B.R. Veeresh [1], R. Suresh[2], S.S. Gowreesh [1]*

[1] Department of Mechanical Engineering, JSS Academy of Technical Education, Bangalore, India.

[2] Department of Mechanical Engineering, Siddaganga Institute of Technology, Tumkur, India.

Received 09.08.2021
Accepted 31.01.2022

Abstract

Welded cylinder structures such as pressure vessels and pipes for transportation have been applied in power stations, aerospace, and shipping industries. The study of weld-induced residual stress is vital in predicting the life of welded cylinder vessels. Depending upon the required diameter and length, they are welded by either circumferential welding or longitudinal welding. In the present work, a sequentially coupled thermal, structural analysis is carried out on circumferential and longitudinal butt weld joints of AH-36 cylinder components. The thermal field distribution and subsequent residual stresses during Gas Tungsten Arc Welding (GTAW) are studied. The moving heat source considered for analysis is based upon Goldak's double ellipsoidal model. The weld-induced axial and hoop stresses are evaluated on both the outer and inner surfaces of the cylinder. The results for circumferential and longitudinal butt weld joints are compared. The magnitude of peak hoop and axial stresses in longitudinal butt weld joints are 45% and 95% higher than in circumferential butt weld joints. The developed analysis model, used to evaluate the thermal histories and residual stresses, is validated with experimental measurements.

Keywords: welding simulation; thin-walled cylinder; thermo-mechanical analysis; residual stress; circumferential weld; longitudinal weld.

*Corresponding author: Veeresh B R, *v.veereshbr@gmail.com*

Introduction

Welded structures have higher joint efficiency and lesser fabricating price. Circumferentially and longitudinally welded cylinders are used in piping fluids at very high temperatures and piping systems carrying steam [1]. Circumferential welding is used when cylinder components have a diameter equivalent to standard sizes. Cylinder components having diameters other than the standard sizes are fabricated by longitudinal welding of rolled metal sheets. Because of welding, residual stresses are induced near the weld area. Residual stresses are stresses that remain in the welded structure even after the heat gradient is removed. The magnitude of residual stresses is almost equal to the yield stress of the base metal [2]. One of the advantages of using longitudinal weld for fabricating large diameter components is cost reduction of up to 30% [3].

The finite element method can be used for the thermo-mechanical analysis of circumferential weld joints in cylinder components to predict the weld-induced stresses [4]. The finite element tool has effectively predicted weld-induced residual stresses and distortions. Many other research works [5-8] are conducted to study the various weld process parameters for circumferential welding, considering different materials of cylinder components. *Afzaal M. Malik et al.* [6], used the ANSYS tool to predict the weld-induced hoop and axial stress in welded pipe structures. *Chunbiao Wu et al.* [7] analyzed the circumferential TIG welding and found that the characteristics of weld-induced residual stresses in cylinder and plate structures are different. *Chin-Hyung Lee et al.* [8] predicted the weld-induced residual stress in circumferential welding of steel pipe structures. They investigated residual stress variations for different cylinder radius to wall thickness ratios. *S. Okano et al.* [9] evaluated weld-induced residual stress and distortion. They found an increase in the spread area of residual stress with an increase in heat input. *R. Lostado et al.* [12] used optimization techniques like genetic algorithms and regression trees combined with the finite element method to optimize the welded structures. The authors have carried out finite element analysis to predict the thermal field and distortion with the help of weld bead geometry. *Susumu Yamada et al.* [13] studied the longitudinally welded cylinder subjected to creep load. Using X-ray spectroscopy, they found that the creep deformation happened faster at HAZ than other locations. *Ruben Lostado Lorza et al.* [14] proposed a finite element model combined with a chaboche kinematic hardening model and isotropic hardening model to predict the residual stresses in V-groove butt weld joints fabricated by gas metal arc welding. They found that the finite element predicted residual stresses are in close agreement with experimental results. The finite element method, in combination with a genetic algorithm, to model a single pass butt weld joint can predict thermal field and deformation more accurately [15]. *F. Miyasaka et al.* [16] developed a welding process model and observed that heat input is vital in maintaining a stable welding bead.

By observing previous research works, it is found that the comparison of thermal histories and residual stresses between the circumferential weld and longitudinal weld joints needs to be carried out. In addition, the literature suggests that with the available advanced computer technology, weld-induced residual stresses can be predicted more precisely. The presented paper performed a numerical study to find the temperature variation, maximum temperature, and residual stresses in circumferential and longitudinal weld joints.

Methodology

Sequentially coupled thermal structural analysis approach is used in the present work and is as shown in Figure 1.

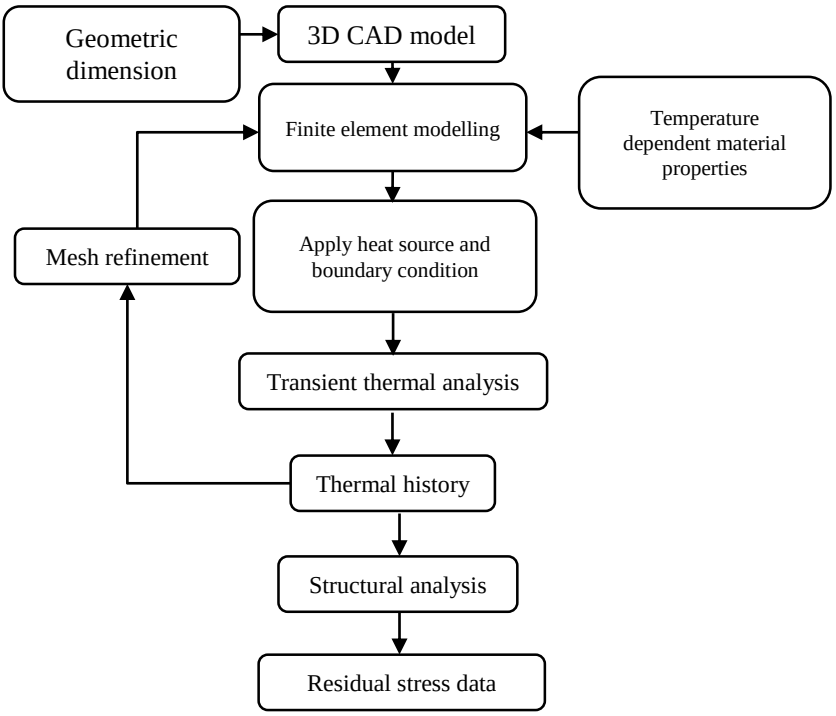

Fig. 1. The methodology followed in the present work.

Finite element modeling

Three-dimensional Finite Element (FE) models of circumferential and longitudinal butt weld joints are developed to measure the temperature and induced stresses. The dimension of the cylinder used during the analysis is 300mm in diameter, 300mm long, and having 3 mm thickness.

In the first step, an investigation is carried out to measure the thermal cycles of the FE model. The measured thermal histories are applied as the thermal load during structural analysis to determine the residual stress distribution.

Contact between the cylinder component_1, weld bead, and cylinder component_2 are defined in both circumferential and longitudinal butt weld joints to facilitate the heat transfer between them, as shown in figure 2. In the beginning, cylinder component_1 is in contact with cylinder component_2, and the heat transfer between them and to surrounding air is the same. With the completion of the welding process, heat transfer (conduction) takes place from the weld bead to cylinder component_1 and cylinder component_2. Also, heat is lost from weld bead and all the free surfaces of the cylinder to surrounding air through convection and radiation. Augmented Lagrangian type of contact algorithm is used to define the contact between the cylinder component_1, cylinder component_2, and weld bead as it gives excellent results [17].

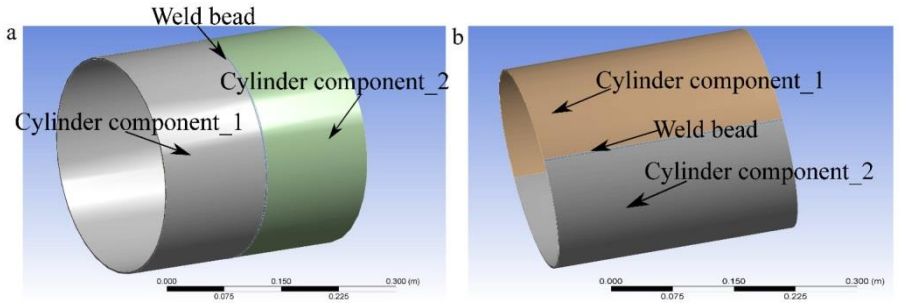

Fig. 2. 3D FE models of a) circumferential and b) longitudinal welds of cylindrical components.

During FE meshing, 1D linear elements are used to represent the weld centerline on which the heat source travels. Along the weld centerline, elements of size 1.8 mm are used during the meshing of both longitudinal and circumferential weld joints. The surface of the FE model from where heat transfer occurs during welding is meshed by 2D quadrilateral elements. Cylinder components and weld bead are meshed by 3D quadrilateral elements. For meshing the cylinder components of both circumferential and longitudinal butt weld joints within a distance of 10 mm from the weld centerline, elements of size 1 mm are used. The distance of 10 mm is measured in a transverse direction on both sides of the weld centerline. For other regions of cylinder components, the size of the elements is 5 mm. Thus, the density of the mesh is higher near the weld centerline. Along with the thickness of the cylinder in both circumferential and longitudinal weld joints, three elements, each having a size of 1 mm, are used for meshing.

Temperature dependent thermal and material properties of AH 36 are considered during analysis and are as shown in Figure 3.

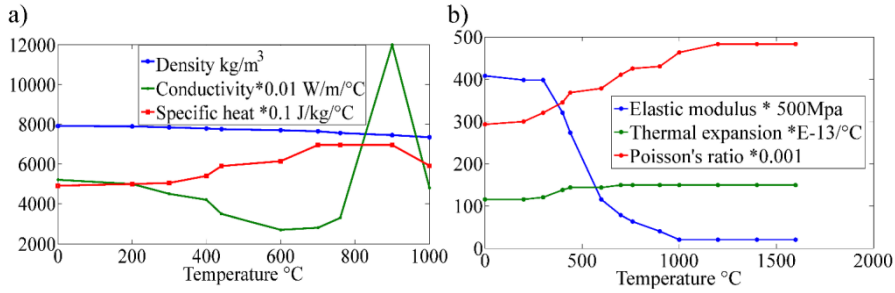

Fig. 3. a) Thermal properties and b) mechanical properties of AH 36 with respect to temperature.

Thermal model

The thermal analysis is conducted to measure the temperature distributions during the welding process. A double ellipsoid heat source model by *Goldak* [10] is considered for representing the heat distribution during the welding process. The heat source model is shown in figure 4. According to Goldak's model, the power density distributions are defined by the governing equations (1) and (2).

$$q_f = \frac{6\sqrt{3}\eta Q f_f}{\pi\sqrt{\pi}a_f bc} exp\{-3\left(\frac{x^2}{a_f{}^2} + \frac{y^2}{b^2} + \frac{z^2}{c^2}\right)\} \quad 1$$

$$q_r = \frac{6\sqrt{3}\eta Q f_r}{\pi\sqrt{\pi}a_r bc} exp\{-3\left(\frac{x^2}{a_r{}^2} + \frac{y^2}{b^2} + \frac{z^2}{c^2}\right)\} \quad 2$$

Where Q is the magnitude of heat input given in equation 3, the heat input is the amount of heat energy transferred for unit length. The portions of heat energy placed in the front and rear quadrants are represented by factors h_f and h_r, respectively. The magnitude of factors h_f and h_r are 1.25 and 0.75, respectively. The shape and size of the heat source model presented in Figure 4 are defined by arbitrary constants a_f, b, c, and a_r. The moving heat source travels on the weld centerline and the calculated volumetric heat flux density is employed to the elements of FE model. The magnitude of the constants in equations 1 and 2 are given in Table 1. Parameters considered during the welding process are mentioned in Table 2. The magnitude of residual stresses induced during welding depends on the magnitude of heat applied. Therefore, the parameters such as current and voltage (power) for welding are considered from the research work carried out by *Afzaal M. Malik et al.* [6]. They have conducted an experimental study on GTAW of cylinder components having 300 mm diameter and 3mm thickness.

The arc travel on the weld centerline during welding is divided into 523 load steps of 0.6 s in the case of the circumferential weld joint. Whereas in the case of the longitudinal weld joint, 166 load steps of 0.6 s are considered.

$$Q = \frac{\eta VI}{n} \quad 3$$

Where I is the current, V is the voltage, η is the efficiency of weld, and n is the arc travel speed.

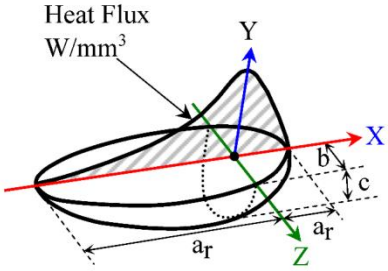

Fig. 4. Double ellipsoid heat source.

Table 1. Values for heat source model.

Parameter	Value in mm
Ellipsoid – front length, a_f	5
Ellipsoid – rear length, a_r	15
Heat source - width, 2b	10
Heat source - depth, c	3

Table 2. Parameters considered during GTAW process.

Parameter	Value
Voltage (V)	12.5
Current (I)	$2*10^2$A
Efficiency (ɳ)	0.8
Speed (n)	3mm/s

Both convective and radiative heat losses are considered during the thermal analysis in evaluating temperature history. The radiation model is based on Steffan Boltzmann relation, and radiative heat transfer is considered from all the free surfaces to ambient air. Heat is lost from all the free surfaces of the FE model, and the governing equation is given by equations (4) and (5).

$$q_{loss} = q_{convection} + q_{radiation} \quad 4$$

$$q_{loss} = [h + \varepsilon\sigma(T + T_{amb})(T^2 + T_{amb}^2)] \times A(T - T_{amb}) \quad 5$$

where h is the convective heat transfer coefficient (25 W/m^2 ^{0}C), A is the surface area, T_{amb} is the ambient temperature (25 ^{0}C), T is the present temperature, σ is Boltzmann constant (5.670 × 10^{-8} W/m^2 K^4), $\mathcal{E}$ is emissivity coefficient (0.8).

Mechanical model

The successive step after thermal analysis is structural analysis. In order to find the weld-induced residual stresses, structural analysis is conducted. After evaluating the temperature distribution, the same FE model is used here, and the mechanical properties considered are temperature dependent. Thermal histories of all the nodes during thermal analysis acts as the thermal load input while von mises criteria is employed. The boundary conditions applied are the restrictions, representing the clamps used to fix the cylinder components during welding. The constraints applied during the welding control the distortion and residual stresses in the cylinder components. High constraint cylinder experiences significant residual stresses and low distortion.

On the other hand, low constraint cylinder experiences lower residual stresses and significant distortion. Hence, constraints play a vital role in producing reliable cylinder structures. In the present case, all the nodes in the thickness direction at 0^0 and 180^0 on both the edges of the cylinder section are constrained in x, y, and z planes and are shown in figure 5.

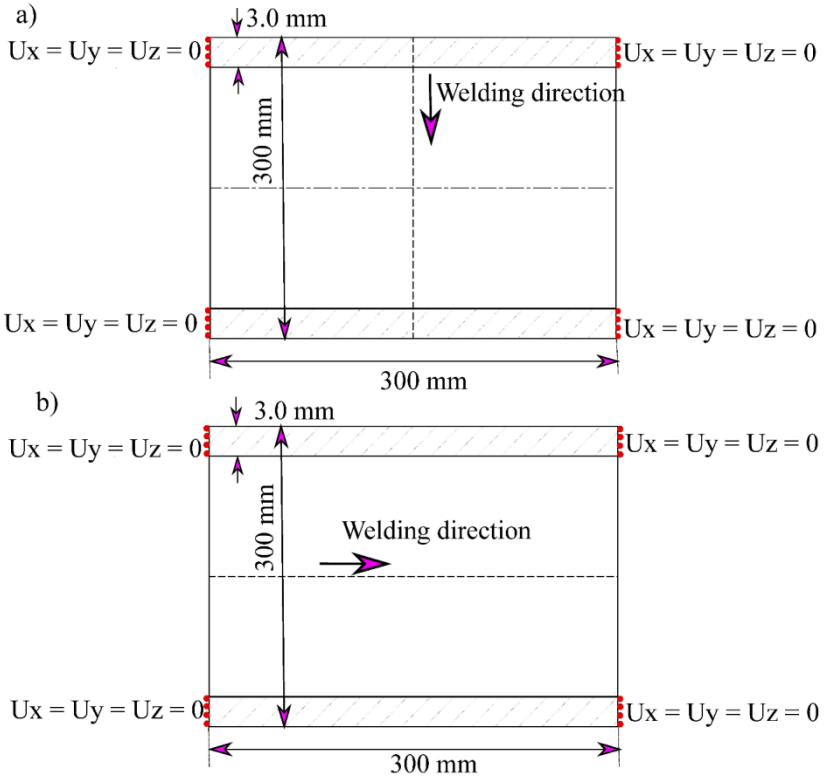

Fig. 5. Boundary conditions applied during structural analysis for a) circumferential weld joint and b) longitudinal weld joint.

During the analysis of circumferential welding, the heat source travels along the circumference of the cylinder. Thus, the weld direction will be normal to the axis of the cylinder. Whereas for longitudinal welding, the heat source travels along the linear direction parallel to the axis of the cylinder.

Validation

The obtained results from the analysis of the circumferential weld joint are compared with the experimental results in the research work carried by *Afzaal M. Malik et al.* [6]. As the residual stresses are induced by uneven cooling, the thermal histories obtained from the FE analysis at different time frames are compared with experimental results. Two criteria, Root Mean Square Error (RMSE) and Mean Absolute Error (MAE), which are defined by equations (6) and (7) are used to compare the temperature data. The magnitude of temperature during circumferential welding at 10mm and 20mm from the weld centerline and at 30° and 90°, respectively, are compared. The distances 10mm and 20mm are measured in the transverse direction to the weld centerline. The locations 30^0 and 90° are measured from the weld start position. The magnitude of temperature on the outer surface of the cylinder at different time frames is tabulated in Table 3.

$$RMSE = \sqrt{\frac{\sum_{j=1}^{V} E_j^2}{V}} \quad 6$$

$$MAE = \frac{\sum_{j=1}^{V} |E_j|}{V} \quad 7$$

Where j = 1,2,3....V, V is the actual number of values, E_j is the difference between the temperature recorded from the experiment and FE analysis at the particular time.

Table 3. Comparison of temperature recorded from the experimental setup and FE analysis.

Sl. No.	Location	Time (s)	Temperature °C (Experimental)	Temperature °C (FEA)	RMSE	MAE
1	10 mm from weld centerline and 30 degree from weld start position	80	890	918	28.19	27.33
2		86	909	850		
3		92	870	899		
4		98	796	818		
5		101	756	784		
6		104	781	763		
7		110	763	730		
8		116	693	715		
9		122	712	689		
10		125	648	669		
11		130	630	654		
12		134	669	630		
1	20 mm from weld centerline and 90 degree from weld start position	80	300	330	36.54	35.91
2		83	385	408		
3		89	472	499		
4		92	496	536		
5		98	527	566		
6		102	529	572		
7		106	533	576		
8		110	536	581		
9		115	534	576		
10		130	520	554		
11		135	512	545		
12		139	501	533		

The residual stresses recorded from the center hole drilling strain gauge method in the research work [6] are compared with FE results. Residual stresses at 45° and 225° at a distance of 10mm from the weld centerline are compared. Locations 45° and 225° are measured from the weld start position. The comparison of FE evaluated residual stresses with experimental measurements in the case of circumferential butt weld joint is presented in Figure 6. The temperature profile and residual stresses obtained during the analysis match closely with the experimental results; thus, the developed FE model is validated.

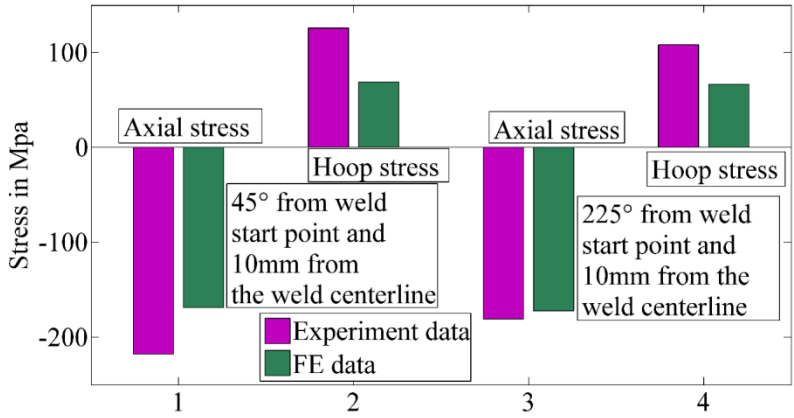

Fig. 6. Comparison of residual stresses obtained from analysis with experimental results on the outer surface, at two different sections.

Results and discussion

Thermal analysis

During the thermal analysis of circumferential welding with a welding speed of 3 mm/s, the heating period along the weld centerline is 314 s. Temperature variations recorded on the outer surface at 108 s are shown in Figure 7. The peak temperature recorded is 1865.2 °C and is observed on the weld centerline. The gradients trailing the heat source indicate the cooling phenomenon of the cylinder components. The temperature profiles during circumferential welding at 78s and 157s are shown in figure 8.

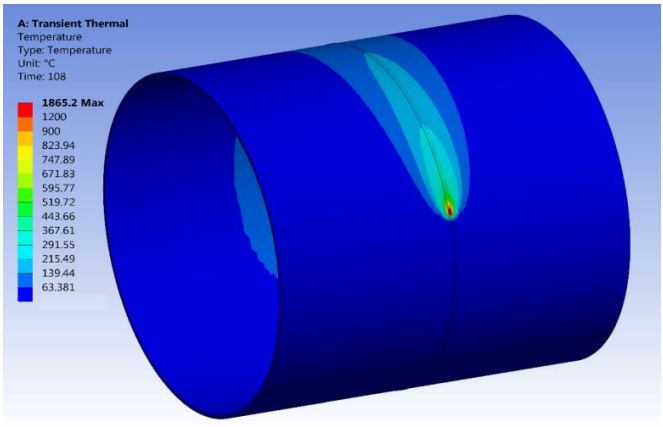

Fig. 7. Temperature profile on the outer surface during circumferential welding.

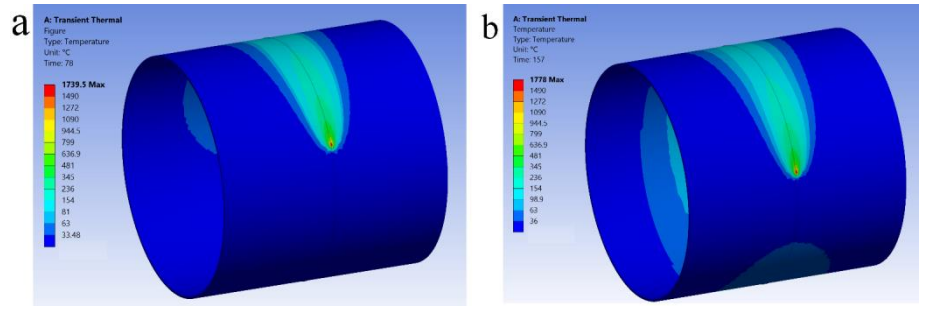

Fig. 8. Temperature profile during circumferential welding at different time frames.

As the results obtained are mesh sensitive, for the FE analysis refinement is necessary. The sequence of analysis is carried out wherein the magnitude of the peak temperature and the corresponding number of elements during each analysis are recorded. The number of elements during FE analysis and the corresponding peak temperatures are shown in Table 4. No change in the magnitude of peak temperature is observed above 54090 elements during circumferential welding.

Table 4. Recorded peak temperature during FE analysis for a different number of elements.

Magnitude of Peak temperature (°C)	Number of Elements
1315.5	30180
1666.9	39360
1800.6	45720
1865.2	54090
1866.3	58319

FE analysis is carried out to find the thermal histories and residual stresses in longitudinal welding. The peak temperature is recorded at 46 s during longitudinal welding and is shown in Figure 9. The temperature profile at 25 s and 50 s is shown in figure 10.

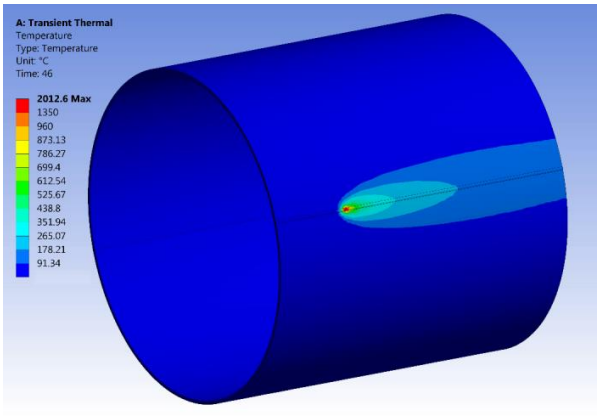

Fig. 9. Temperature profile on the outer surface during longitudinal welding.

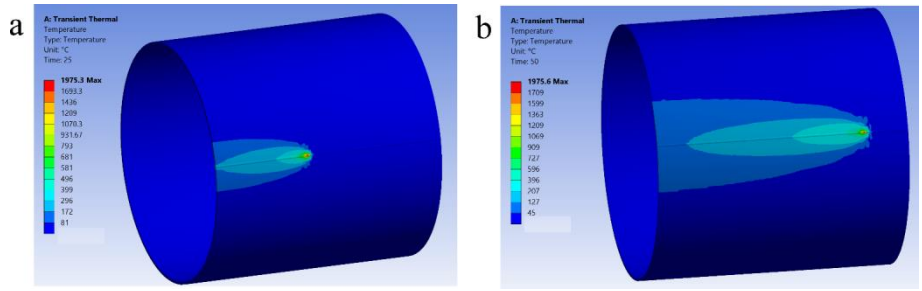

Fig. 10. Temperature profile during longitudinal welding at different time frames

From figures 7 and 9, the maximum temperatures during the analysis are 1865.2 °C and 2012.6 °C for circumferential and longitudinal butt weld joints, respectively. The peak temperatures are observed on the weld centerline. By considering the arc travel speed of 3 mm/s, the time taken to weld 150 mm in case of longitudinal welding is 50 seconds. Whereas in the case of circumferential welding, the time taken is 157 seconds for the heat source to travel 180°. Thus, the magnitude of temperature recorded on the weld centerline and other locations for longitudinal welding is higher than circumferential welding.

Because of convection and radiation, the welded cylinder vessel cools down to ambient temperature. The temperature variation during circumferential and longitudinal welding at different time frames is shown in Figures 11 and 12. The temperature variation is considered along the axial direction at 135° from the weld start location for the circumferential weld joint. For longitudinal weld joint, temperature variation is considered circumferentially at 135 mm from the weld start location. The magnitude of temperature is maximum at the welding arc position and decreases as the arc crosses the location. The analysis is carried out for 6000 seconds so that the complete cylindrical vessel cools to ambient temperature.

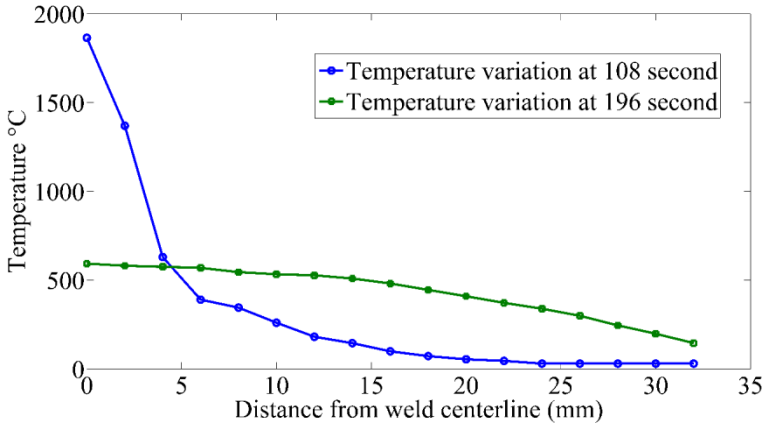

Fig. 11. Temperature variation in the circumferential weld joint at different time frames.

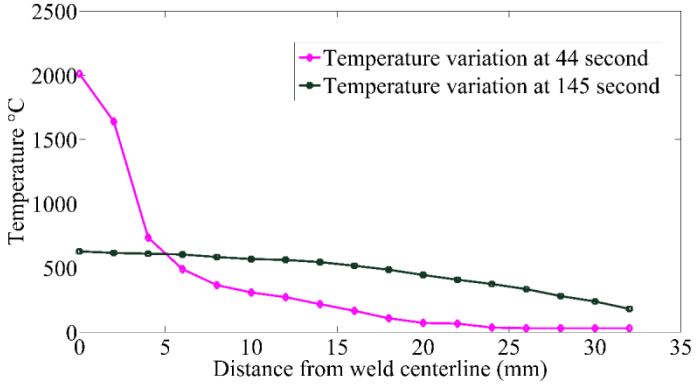

Fig. 12. Temperature variation in the longitudinal weld joint at different time frames.

Structural analysis

Stress parallel to the weld centerline is hoop stress, and the stress along the axis of the cylinder is axial stress in the case of circumferential weld joints. Similarly, stress parallel and normal to weld centerline are axial and hoop stress, respectively, in the case of longitudinal weld joints.

Weld-induced stresses are evaluated on both the inner and outer surfaces of the cylinder during structural analysis. The residual stress variations are evaluated at 180° and at 150 mm cross-sections for circumferential and longitudinal weld joints, respectively. The axial stress variations are shown in figures 13 and 14. Similarly, hoop stress variations are shown in figures 15 and 16. These residual stresses recorded are in the direction normal to the weld centerline for both circumferential and longitudinal weld joints. It can be noted that the sections 180° and 150 mm are considered circumferentially and axially for circumferential and longitudinal weld joints, respectively. It is observed that the stress distribution profiles for circumferential and longitudinal butt weld joints are similar to some extent. But the magnitude of stresses is higher for longitudinal butt weld joints.

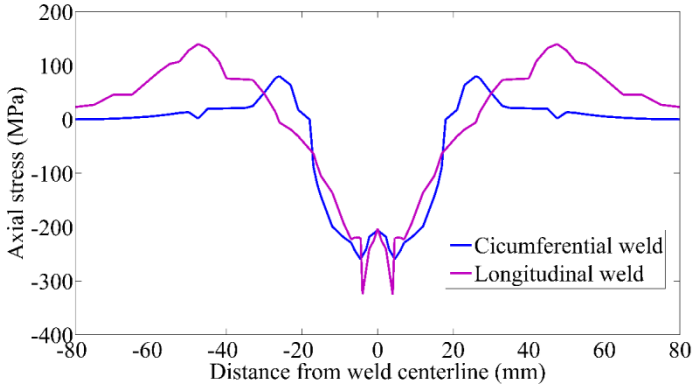

Fig. 13. Residual axial stress distribution on the outer surface for circumferential and longitudinal weld butt joints.

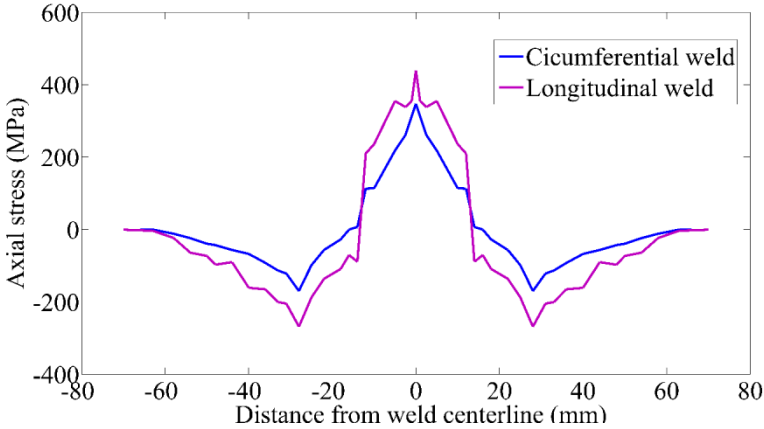

Fig. 14. Residual axial stress distribution on the inner surface for circumferential and longitudinal weld butt joints.

From figure 13, residual axial stress obtained on the outer surface is compressive in the vicinity of the weld region. The stress reverses to tensile at the section 20 mm away from the weld centerline. Then the tensile stress magnitude increases until around 25 mm and 45 mm for circumferential and longitudinal butt weld joints, respectively. It is observed that the stress magnitude gradually becomes nil at the locations near the cylinder edges.

The axial stress on the inner surface of the cylinder, for both circumferential and longitudinal butt weld joints, is tensile at the weld location. The stress reverses to compressive at the section 15 mm away from the weld centerline. Residual axial stress is almost nil at the cylinder edges.

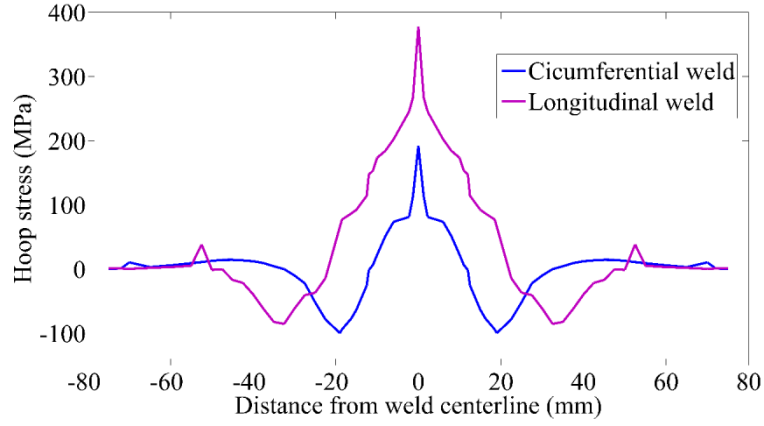

Fig. 15. Residual hoop stress distribution on the inner surface for circumferential and longitudinal weld butt joints.

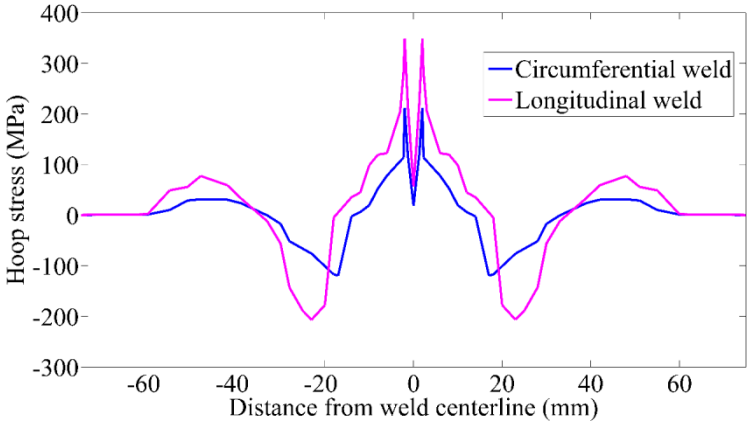

Fig. 16. Residual hoop stress distribution on the outer surface for circumferential and longitudinal weld butt joints.

From figures 15 and 16, it is found that the residual hoop stresses are tensile near the weld centerline for both circumferential and longitudinal butt weld joints. The hoop stress reverses to compressive around a distance of 15 mm and 20 mm from the weld centerline for circumferential and longitudinal butt weld joint, respectively. Hoop stress magnitude reduces to zero at the cylinder edges.

The magnitude and locations of peak residual stresses induced in circumferential and longitudinal weld joints are shown in table 5.

Table 5. The magnitude of residual stresses.

Type of weld joint	Type of residual stress	Magnitude of peak stress	Location of peak stress
Circumferential	Axial	345 Mpa	Weld center
	Hoop	210 Mpa	2 mm from Weld center
Longitudinal	Axial	435 Mpa	Weld center
	Hoop	375 Mpa	Weld center

Because of internal pressure in the thin-walled cylinder, hoop and axial stresses are induced. The hoop stress will be two times larger in magnitude than the axial stress. This pressure induced hoop stress sums up the residual hoop stress in the case of welded cylinder vessels. From table 5, it is found that the magnitude of peak hoop stress found in longitudinal butt weld joint is significantly higher than circumferential butt weld joint. In the case of longitudinal weld joints, the magnitude of peak hoop stresses is 135 MPa and 185 MPa higher on the outer and inner surfaces, respectively. Therefore, longitudinal butt weld joints are not advisable for fabricating cylindrical components.

Conclusion

FE method is used to calculate the temperature and residual stress variations in circumferential and longitudinal butt weld joints of cylinder vessels. By observing the results following are the conclusions drawn:

- The thermal histories and residual stress distributions for circumferential butt weld joint obtained from the FE analysis matches closely with the experimental results available in the literature. The same model is being implemented in evaluating the weld-induced axial and hoop stresses in the longitudinal butt weld joint.

- The magnitude of temperature observed on the weld centerline and other locations for the longitudinal butt weld joint is higher than the circumferential butt weld joint.

- The residual hoop stress induced on the outer and inner surfaces is maximum near the weld centerline and is tensile.

- Difference is observed in the magnitude of axial and hoop stresses between circumferential and longitudinal butt weld joints. The peak hoop stress induced in the longitudinal butt weld joint is significantly higher.

- The obtained results suggest that the longitudinal butt weld joints are not desirable for fabricating cylinder components, as it reduces the service life.

Acknowledgment

The Authors appreciatively acknowledge Siddaganga Institute of Technology, Tumkur for the valuable support provided for the research work.

References

[1] A. Kermanpur, M. Shamanian, V. Esfahani Yeganeh: J Mater Process Technol, 199 (2008) 295-303.
[2] R.H. Leggatt: Int J Pressure Vessels Piping, 85 (2008) 144-151.
[3] Segle P, Tu S-T, Storesund J, Samuelson LA: Int J Pressure Vessels Piping, 66 (1996) 199-222.
[4] Tso-Liang Tenga, Peng-Hsiang Chang: Int J Pressure Vessels Piping, 75 (1998) 548-556.
[5] Naeem Ullah Dar, Ejaz M. Qureshi, M.M.I Hammouda: J Mech Sci Technol, 23 (2009) 46-54.
[6] Afzaal M. Malik, Ejaz M. Qureshi, Naeem Ullah Dar, Iqbal Khan: Thin-Walled Struct, 46 (2008) 199-222.
[7] Chunbiao Wu, Jae-Woong Kim: Thin-Walled Struct, 132 (2018) 421-430.
[8] Chin-Hyung Lee, Kyong-Ho Chang: Mater Sci Eng, 487 (2008) 210-218.
[9] S. Okano, M. Tanaka, M. Mochizuki: Sci Technol Weld Joining, 16(2013) 209-214.
[10] John goldak, Aditya chakravarti, Malcolm bibby: Metall Mater Trans B, 15B (1984) 299-305.
[11] J.A. Goldak, M. Akhlaghi: Computational Welding Mechanics, first ed. Springer US, New York, 2005, 22-35.
[12] R. Lostado, R. Fernandez Martinez, B.J. Mac Donald, P.M. Villanueva: Integr. Comput Aided Eng, 22 (2015) 153-170.
[13] S. Yamada, M. Yaguchi, T. Ogata: Mater Sci Eng, A 560 (2012) 450-457.
[14] R.L. Lorza, M.C. Bobadilla, M.Á.M. Calvo, P.M.V. Roldán: Metals, 7 (2017) 1-25.

[15] R.L. Lorza, R.E. García, R.F. Martinez, M.Á.M. Calvo: Metals, 8 (2018) 1-25.
[16] F. Miyasaka, Y. Yamane, T. Ohji: Sci Technol Weld Joining, 10 (2013) 521-527.
[17] Serhan Sezer: Louisiana State University, Master's Theses, 2005.
[18] S.Íñiguez-Macedo, R. Lostado-Lorza, R. Escribano-García, M.Á. Martínez-Calvo: Materials, 12 (2019) 1-20.
[19] A. Mitraa, N. Siva Prasadc, G.D. Janaki Ram: J Mater Process Technol, 229 (2016) 181-190.
[20] B.Q. Chen, M. Hashemzadeh, Y. Garbatov, C. Guedes Soares: Int J Mech Mater Des, 11 (2014) 439-453.